

MTDT: A Multi-Task Deep Learning Digital Twin

Nooshin Yousefzadeh, Rahul Sengupta, Yashaswi Karnati, Anand Rangarajan, and Sanjay Ranka
University of Florida, Gainesville, FL, USA

Abstract—Traffic congestion has significant impacts on both the economy and the environment. Measures of Effectiveness (MOEs) have long been the standard for evaluating traffic intersections' level of service and operational efficiency. However, the scarcity of traditional high-resolution loop detector data (ATSPM) presents challenges in accurately measuring MOEs or capturing the intricate spatiotemporal characteristics inherent in urban intersection traffic. To address this challenge, we present a comprehensive intersection traffic flow simulation that utilizes a multi-task learning paradigm. This approach combines graph convolutions for primary estimating lane-wise exit and inflow with time series convolutions for secondary assessing multi-directional queue lengths and travel time distribution through any arbitrary urban traffic intersection. Compared to existing deep learning methodologies, the proposed Multi-Task Deep Learning Digital Twin (MTDT) distinguishes itself through its adaptability to local temporal and spatial features, such as signal timing plans, intersection topology, driving behaviors, and turning movement counts. We also show the benefit of multi-task learning in the effectiveness of individual traffic simulation tasks. Furthermore, our approach facilitates sequential computation and provides complete parallelization through GPU implementation. This not only streamlines the computational process but also enhances scalability and performance.

Index Terms—Deep Learning, Multi-task Learning, Graph Neural Networks, Convolutional Neural Networks, Traffic, Intersection, ATSPM, MOEs.

I. INTRODUCTION

Traffic congestion in urban areas impacts efficiency, economics, environment, safety, and overall life quality. Measures of Effectiveness (MOEs) provide a benchmark of longitudinal perspectives to quantify the level of service and evaluate the performance of transportation systems. The employment of MOEs is also useful for optimizing the signal timing plan of intersections and the overall traffic flow accordingly. Common MOEs for urban traffic control include factors such as queue length, travel time, waiting time, number of stops, vehicle throughput, average speed, fuel efficiency and emissions, safety, equity, adaptability to demand, public satisfaction, accessibility, etc. Depending on the specific municipal goals and priorities, a combination of MOEs can be used to effectively evaluate the urban traffic control system. This study includes but is not limited to two commonly used MOEs: 1- Queue Length: Distance from the stop bar to the tail of the last vehicle stopped in any traffic lane, and 2- Travel Time: The time necessary to traverse any route connects any two points of interest.

Microscopic simulators e.g., VISSIM, SUMO, and AIM-SUN fail to generalize to arbitrary topology and infrastructure of traffic urban roadways without painstakingly (re)drawing

base maps and (re)setting traffic simulation parameters. Some data sources e.g., GPS, Video, BlueTooth, DSRC, etc. are normally sparse with privacy and ownership restrictions [19]. Advanced sensing technologies such as induction loop detectors (ATSPM), make high-resolution loop detector traffic data widely available, although they fail to provide enough information for MOEs estimation by themselves. The computation of MOEs is specific to several tempo-spacial factors such as intersection characteristics(e.g., topology, lane configuration), traffic pattern (e.g., inflow traffic and turning-movement counts, signal timings, and traffic conditions (e.g., driving behaviors).

Existing analytical methods of estimating MOEs from ATSPM either use vehicle conservation input-output algorithms based on counting vehicle flow over advance and stop-bar detectors [18] or Lighthill's shockwave-based methods that identify breakpoints in the detector actuation waveforms [22]. Although, both of them are sensitive to the placement of detectors and limited to the localized training datasets. Machine learning methods use either GPS trace data [5] that are too coarse in recording dissipation trends, or ATSPM for cycle-wise MOEs which is not based on real-world traffic conditions due to the random vehicle flow and road networks without explicit left-turn buffers. Recently, some deep learning methods have employed geometric deep learning [20] and graph convolution networks [7] to extract cycle-wise MOEs, although these approaches still fail to generalize the local traffic conditions and road geometries, also their reconstructed MOEs have as low resolution as approach level.

We propose a Multi-Task Deep Learning-based (MTDT) digital twin of intersections to address the aforementioned shortcomings. This model is trained on real-world data obtained from high-resolution induction loop detectors (ATSPM), capturing varying traffic patterns encompassing a wide range of configurable parameters, thus generating potentially viable counterfactual traffic scenarios. MTDT builds upon the previous work by Yousefzadeh et al. [23], extending it to create an accurate and reliable multi-purpose digital twin. The main difference between them is that [23] introduces two individual deep learning-based digital twins that utilize graph neural networks to make a lane-wise estimation of either exit or inflow waveforms at any direction of an arbitrary intersection. We use a multi-task learning paradigm to combine graph convolution for learning primary lane-wise traffic waveforms with time series convolution for learning secondary multi-directional MOEs based on primary results for an arbitrary urban traffic intersection, all at the same time. While maintaining a straightforward design, our model

emphasizes the advantages of multi-task learning in traffic modeling. Although additional complexities could potentially enhance feature learning, we have prioritized simplicity to underscore the benefits of multi-task learning in modeling traffic flow dynamics. By consolidating the learning process across multiple tasks, MTDT demonstrates reduced overfitting, increased efficiency, and enhanced effectiveness through the sharing of representations learned by different tasks. An overview of our model is depicted in Figure 1, where orange-colored objects represent the inputs of the model, including stop-bar loop detector waveforms and signal timing plans (additionally are present driving behavior parameters and turning-movement counts features), while blue-colored objects represent the outputs of the model, including exit and inflow waveforms at each traffic lane, maximum queue length at each traffic phase, and travel time distribution at each traffic phase. Further details regarding the definition and computation of these MOEs are provided in Section IV. Traffic Data Generation.

The following are the key contributions of our work:

- MTDT jointly estimates fine-grained and lane-wise exit and inflow waveform time series, along with accurate travel time distribution and maximum queue lengths associated with every phase of the movement. The model's adaptability and responsiveness to the spatiotemporal intricacies of traffic dynamics are evident in its utilization of input parameters such as relevant driving behavior metrics, signal timing plans, turning movement counts, and signal timing plan parameters, among others.
- Using our digital twins, it becomes feasible to accurately and reliably predict the impact of loop detector waveforms, signal timing plans, driving behavior parameters, and turning movement counts on lane-wise platoons and related MOEs. Importantly, this predictive capability is computationally faster than microscopic simulators, thanks to the utilization of GPU-based processors. The methodologies proposed in our digital twins incur $O(1)$ sequential computation and can be entirely parallelized using cost-effective GPU computation.
- The findings of this study hold significance to extend to corridor and network level digital twins, and make benefits towards data-driven traffic control design and safety management, particularly in the context of smart intersections operating within highly dynamic environments.

We designed several experiments, whose findings aim to showcase the feasibility and efficacy of our multi-tasking approach in designing a deep learning-based and multifaceted digital twin for intersections. We introduce two variants of our digital twin and compare our model with them and with our previously introduced TQAM [15] digital twin. The results of the experiments, underscore the versatility of our proposed digital twin, demonstrating its ability to not only generalize estimations across various intersection typologies and characteristics, but also successfully simulate ATSPM waveforms at lane level, and accurately estimate several Measures of Effectiveness (MOEs) in both time series

and distribution forms at phase (lane-group) level for every approach (movement direction) within an urban intersection.

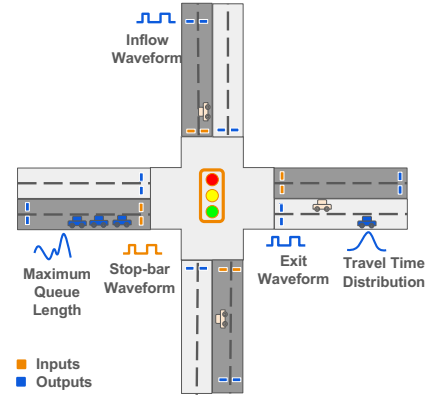


Figure 1: The inputs and outputs of Deep Multi-Task Learning Digital Twin. We simulate the ATSPM time series waveform along with waveform or histogram of several MOEs within 8-phase standard NEMA phasing intersections. MTDT simultaneously estimates downstream exit waveforms of every outflow lane in all directions and upstream inflow waveforms of every inflow lane in all directions with an estimation of instant maximum queue length and travel time distribution associated with each phase of movement for an intersection with arbitrary topology and traffic conditions.

The rest of the paper is organized as follows: Section VI provides an overview of related work, discussing various techniques employed for traffic state estimation. Section III outlines the architecture of our proposed digital twin. Finally, in Section V, we assess and compare the performance of our model through a series of experiments.

II. PROBLEM DEFINITION

This section extends the basic concepts and formal definitions introduced in our previous work to formulate our research problem in this study. For simplicity, the notations and terminologies are considered to be consistent. Detailed descriptions of the notations used in this study are presented in Table 1.

Definition 1. Simulation Record: This term refers to a record of a simulation run represented as a tuple of intersection ID, signal waveform sig , turn-movement counts vector tmc , driver behavior vector drv , lane-wise stop-bar loop detector waveforms stp , exit loop detector waveforms ext , and inflow loop detector waveforms inf , and multi-directional queue length waveforms ql , and travel time histograms tt .

Definition 2. Simulation Graph: This term refers to a single graph data item constructed using a standardized and generic structure, to represent a single traffic scenario occurring at a certain intersection. In this study, we construct two types of *Simulation Graph* for each intersection j from each single *Simulation Record* s each with its own attributes and structure to model exit traffic waveforms ($g_{s,j} = (V, E, X, Z)$) and inflow traffic waveforms ($g'_{s,j} = (V', E', X', Z)$). Both of them are directed bipartite graphs that connect each stop-bar loop detector to corresponding exit detectors in the node set V or to inflow detectors in the node set V' . with edge features $Z = [sig_{j,w}, tmc_j, drv_j]$ at each graph defined as the

concatenation of the signal timing plan time series, turning-movement counts vectors, and driving behavior parameters.

Notation	Description	Aggr	Size	Type
j	Intersection	-	1x9	String
stp	Waveform at Stop-bar detector	5 sec	48x80	Integer, 0-8
ext	Waveform at the exit of the intersection	5 sec	16x80	Integer, 0-8
inf	Waveform upstream the intersection	5 sec	12x80	Integer, 0-8
ql	Queue length time series	5 sec	8x80	Integer, 0-1200
tt	Travel time histogram	5 sec	8x200	Integer, 0-700
sig	Signal timing state information	5 sec	8x80	Binary
drv	Driving behavior parameters	2400 sec	1x9	Float, 0-30
tmc	Turning-movement counts ratio	2400 sec	35x35	Float, 0-1
w	Size of the prediction window	-	1	Integer, 0-150
s	Single simulation recorded by SUMO	5 sec	-	Multiple
A	Common lane-connectivity for M_{ext} module	-	2x22	Binary
A'	Common lane-connectivity for M_{inf} module	-	2x72	Binary
v	multivariate time series for queue length estimation	5 sec	1x7x80	-
v'	multivariate time series for travel time estimation	5 sec	1x7x80	-
M_{ext}	GAT module for exit waveforms estimation	-	-	torch.nn.Module
M_{inf}	GAT module for Inflow waveforms estimation	-	-	torch.nn.Module
M_{ql}	CNN module for queue length estimation	-	-	torch.nn.Module
M_{tt}	CNN module for travel time estimation	-	-	torch.nn.Module

TABLE 1: Summary of the notations and their definitions.

III. PROPOSED MODELS

The Multi-task Deep Learning Digital Twin (MTDT) is designed to grasp various facets of intersection-level traffic flow dynamics simultaneously. MTDT is jointly optimized to learn four sets of joint tasks. The general architecture of our digital twin is composed of two primary modules that yield base learning representations, and two secondary modules that use the representations learned by primary modules to learn their own tasks and improve the learning process of primary tasks as well by the sharing of their representations. For a comprehensive understanding of MTDT's architecture, refer to the overview depicted in Figure 2. Here, as described in Table 1, M_{ext} and M_{inf} represent GAT modules that execute exit waveforms and inflow waveforms estimation respectively; while M_{ql} and M_{tt} represents CNN modules that execute queue length time series and travel time distribution estimation respectively. The output of primary tasks of size 16×80 for the exit task and 12×80 for the inflow task are aggregated to 8 lane groups (phase of movement) to the size 8×80 before being fed as input to the secondary tasks.

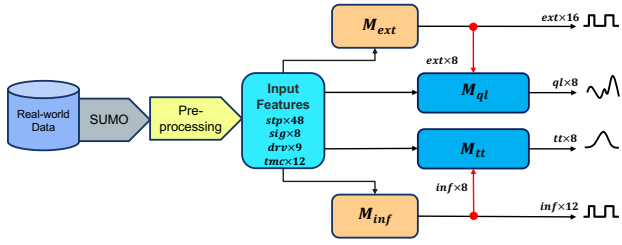


Fig. 2: **Overview of the architecture of MTDT.** The architecture of the proposed Multi-componential digital twin framework contains two types of modules. GAT modules (light orange colored) execute primary tasks, which aggregated outputs are used as input to secondary tasks executed by CNN modules (dark blue colored). Red-colored arrows are activated only in inference mode.

The MTDT pipeline comprises two distinct types of modules: Graph Attention Networks (GATs) [17] modules, including M_{ext} and M_{inf} , dedicated to the primary task of estimating loop detector waveforms, and Convolutional Neural Networks (CNNs) [8] modules, including M_{ql} and

M_{tt} , geared towards secondary tasks such as estimating Measures of Effectiveness (MOEs) like maximum queue length and travel time distribution. More specifically, GAT modules, namely M_{ext} and M_{inf} , excel at precise, lane-specific estimations of waveform time series for vehicle platoons approaching and departing the target intersection. They meticulously consider instantaneous spatiotemporal factors like turning movement counts, driving behavior parameters, and signal timing plans. Subsequently, CNN modules, such as M_{ql} and M_{tt} , utilize the outputs from primary modules alongside instantaneous spatiotemporal characteristics of the target intersection to estimate MOEs like maximum queue length and travel time distribution. This design ensures adaptability without restrictive assumptions, making the digital twin easily instantiated for various secondary tasks related to traffic dynamics.

The underlying principle of this architecture lies in extracting and leveraging valuable additional information from diverse aspects of the same phenomenon, resulting in enhanced performance and more comprehensive outcomes. Proper normalization techniques tailored to each task are employed to enhance the performance of both primary and secondary tasks collectively.

A. Exit Module

Exit subnetwork module M_{ext} is an attentional graph neural network (GAT) with an imputation mechanism, as introduced in [23] to perform the primary task of exit waveform time series ext estimation. Here, the input data is fed in the form of *Exit Simulation Graphs* with a common connectivity matrix and masked node features to connect a total number of 16 exit loop detectors' ext waveform time series (for 4 outflow lanes for each approach) to the total number of 48 stop-bar loop detectors' stp waveform time series as in a general topology of an arbitrary up to 4-way intersection. This module consists of a GATConv [17] message passing layer following a single fully connected linear layer parameterized by weight matrix $B \in \mathbb{R}^{w \times N}$ and activated by a ReLU function to generate and propagate messages of hidden representation inflow lanes to any other connected outflow lanes within the intersection network. The attention mechanism in GATConv is a SINGLE-layer feed-forward neural network, parameterized by a weight vector $a \in \mathbb{R}^{N \times w}$ with ReLU non-linearity.

$$a_{ij} = \text{ReLU}(a^T [W h_i \| W h_j])$$

Through this technique, GATConv implicitly specifies and integrates the attention coefficients signifying the importance of each stp waveform time series to each ext waveform.

$$\alpha_{ij} = \text{Softmax}_j \left(\frac{\exp(e_{ij})}{\sum_{k \in N_i} \exp(e_{ik})} \right)$$

Where N_i is the connected (neighboring node) lanes of each lane i in the intersection's graph representation. A fully-connected layer activated by a ReLU function is applied on the output of the GATConv layer to impute missing

(unobserved) time series waveforms for exit loop detectors ext within reconstructed input feature matrix $\hat{X} \in \mathbb{R}^{N \times w}$.

B. Inflow Module

Inflow subnetwork module M_{inf} is an attentional graph neural network (GAT) with an imputation mechanism, as a simplified version of multi-layer graph neural network [24] solution introduced in [23]. This module is responsible for performing the primary task of inflow waveform time series inf estimation. The difference between M_{ext} and M_{inf} is that the same GATs module architecture is adopted to perform a different primary task. Here, GATConv implicitly specifies and integrates the attention coefficients denoting the importance stp waveform time series to each inf waveform using a different graph representation of an intersection that connects each of 12 inflow loop detectors' ext waveform time series (for 3 inflow lanes for each approach) to the total number of 48 stop-bar loop detectors' stp waveform time series as in a general topology of an arbitrary up to 4-way intersection. In this setting, this GATs module can impute missing (unobserved) time series waveforms for exit loop detectors inf within reconstructed input feature matrix $\hat{X} \in \mathbb{R}^{N' \times w}$.

C. Queue Length Module

Queue Length subnetwork module M_{ql} is a multi-output 1D convolutional neural network (CNN) to perform the secondary task of maximum queue length waveform time series ql estimation. Here, the input data is fed in the form of *Multivariate Time series* $v_{s,j}$ of size (8, 7, 80) each time step for each of 8 traffic phase, pair 7 variables including exit waveform time series ext estimated by M_{ext} with stp , driving behavior parameters drv , and signal timing plans sig to capture appropriate and instant spatiotemporal characteristics of urban traffic intersections. In this setting, for simplicity reasons, only the three most effective driving behaviors i.e., accel, lcCooperative, minGap in traffic dynamic of intersection, based on SHAP analysis of the Average impact of features on the magnitude of estimation in [23], are included. The architecture of the CNNs module consists of 3 Conv1d layers each followed by a MaxPool1d layer and flattening layer before being fed into a fully connected layer activated by a ReLU non-linearity to simultaneously generate a set of 8 outputs as an estimation to maximum queue length waveform time series for every phase of target standard NEMA eight-phasing intersection.

D. Travel Time Module

Queue Length subnetwork module M_{tt} is a multi-output 1D convolutional neural network (CNN) to perform the secondary task of travel time histogram tt estimation. Here, the input data is fed in the form of *Multivariate Time series* $v'_{s,j}$ of size (8, 7, 80) each time step for each of 8 traffic phases, pair 7 variables including inflow waveform time series inf estimated by M_{inf} with stp , driving behavior parameters

drv , and signal timing plans sig to capture appropriate and instant spatiotemporal characteristics of urban traffic intersections. The architecture of this module remains the same as the M_{ql} module.

E. Loss Construction

Multi-task Deep Learning Digital Twin (MTDT) is trained on numerous realistic traffic scenarios simulated across eight distinct intersections. It takes stop-bar high-resolution loop detector data, driving behavior parameters, signal timing plan parameters, and turning movement counts as inputs to generate exit and inflow time series waveforms for each lane of movement, alongside maximum queue length time series and travel time distribution for each phase of movement.

During the multi-tasking learning process in MTDT, information is extracted from four sources shown as $M = \{M_{ext}, M_{inf}, M_{ql}, M_{tt}\}$ learning modules. These modules cater to four different yet interconnected tasks denoted as $T = \{ext, inf, ql, tt\}$ each yielding an output $\{y_t\}_{t \in T}$ and a computed loss value $\{l_t\}_{t \in T}$. The model undergoes simultaneous training across all tasks, with losses applied to facilitate learning across the entire spectrum. The final loss $L = \sum_{t \in T} l_t$ is computed as the summation of partial loss values obtained from optimizing all primary and secondary learning tasks.

In the training phase, the learning process for both primary and secondary tasks operates independently while being supervised by log information generated by the SUMO micro-simulator for each target variable. The input information is represented either as *Simulation Graphs* for GATs modules handling primary tasks or as *Multivariate Time Series* for CNNs modules addressing secondary tasks. While, in the inference phase, the secondary tasks are facilitated by information derived from primary tasks involved in constructing their inputs (i.e., shown by the activation of red-colored arrows in Figure 2). The output of secondary modules in inference mode is generated by performing a 1D convolutional operation on the resulting 1D *Multivariate Time Series*. It's worth noting that this study employs a simplified design to illustrate the benefit of this generic approach, more complex architectures with improved feature learning might lead to better results.

In the multi-tasking paradigm, consistency across the scale of outputs scales is important. In this experiment, a traffic scenario for a certain intersection includes several variables: ext and inf are time series with a range of 0-8 in the unit of number of vehicles, while ql is time series with a range of 0-1200 in the unit of meter, and tt is a histogram with range 0-700 in the unit of seconds. To optimize the generalization of the optimization scheme within our multi-task learning paradigm, we employ appropriate experimental normalization techniques tailored to each task to ensure equal weighting (prioritization) of partial loss values computed by different tasks. We use the min-max normalization technique for y_{ext} and y_{inf} and y_{tt} and log normalization for y_{ql} . For each normalization and scaling formula, a counterpart denormalization function is utilized to transform $\{\hat{y}_t\}_{t \in T}$

back to the original scale before computing error values for estimations.

$$\hat{y}_t = \text{Denorm}_t(\text{M}_t(\text{Norm}_t(X_t)))$$

The choice of loss function for each task also is aligned with the data type and task objectives. We use the mean squared error loss function for time series and cross-entropy loss function for histogram optimization treating the number of bins as the number of labels for its ordinal categorical variable.

The model is trained on the train portion (75% split of data), and a grid search algorithm is employed to fine-tune regularization hyperparameters on the 15% split of the validation portion. The model is evaluated on to the test partition and the error values are reported for the best-performing model across 100 epochs of training.

In this study, we deliberately maintain a simplistic architecture to showcase the advantages of this learning paradigm in our application, introducing subtle additional complexities could potentially yield improved results through enhanced feature learning capabilities.

IV. TRAFFIC DATA GENERATION

Our dataset is based on over 400,000 simulation hours of SUMO data. A 9-intersection urban corridor located in a large metropolitan region in the United States of America was chosen. We reiterate the important points here; more details on the dataset are provided in [23].

We use real-world ATSPM (loop detector) data with sparse WEJO (GPS) probe trajectory data sources to generate an approximate Origin-Destination probability matrix. This provides insight into the probability of a vehicle originating from a specific location reaching various valid destinations. SUMO tool od2trips is used to generate route files for the simulation.

Building upon the configuration parameters and the range of variation detailed in Supplementary Table 1 of [23], we augment our data generation process with additional processing. This enhancement enables the collection of several Measures of Effectiveness (MOEs) corresponding to the state of traffic flow across various simulated counterfactual traffic scenarios.

For signal timing plans, we use Ring-and-Barrier operation with a common cycle length. Parameters such as the minimum/maximum green times, yellow times, and red times for the intersections are based on signal timing sheets. However, we do vary the common cycle lengths and barrier times. A random common cycle length is chosen between 120 seconds and 240 seconds. Once this is selected, random signal cycle offsets are chosen for each intersection separately. A random barrier time is chosen. Driving behavior parameters (such as acceleration, deceleration, emergency braking, minimum gap between vehicles, headway, lane-changing parameters, etc.) are also varied. Finally, with some additional processing, we get the outputs of several Measures of Effectiveness(MOEs) to measure the state of traffic flow generated at counterfactual scenarios.

Queue Length. The maximum queue length time series for each approach or traffic phase represents the instant magnitude of the maximum queue length in the unit of meter aggregated at a 5-second bucket resolution. In order to get the variation of queue length over time, we take the maximum queue length seen for a group of lanes associated with each phase of movement at a 5-second resolution. This is obtained directly by parsing SUMO log files and tracking queue lengths on a per-second basis. For the through-lanes (i.e. lanes serving the even number phases 2/4/6/8), we take the maximum queue lengths seen in 5 seconds across all (a) the 1-hop lanes serving the through-lanes and (b) 2-hop lanes w.r.t. the intersection. We then sum these two maximum queue lengths (a) and (b) to get the overall queue length. Broadly, this number gives the maximum possible queue length that any of the lanes belonging to the through-lanes, might experience. For the left-lanes (i.e. lanes serving the odd number phases 1/3/5/7), we take the maximum queue lengths seen in 5 seconds across all (a) the 1-hop lanes serving the left-lanes and (b) the left-most 2-hop lane w.r.t. the intersection. We then sum these two maximum queue lengths (a) and (b) to get the overall queue length. The reason for choosing only the left-most 2-hop lane for (b) is that it is assumed that many vehicles that wish to take a left-turn, would have begun changing into the left-most lane in anticipation of the start of the left-turn buffer. Thus, the maximum queue length should take into account the left-most lane.

Intersection Travel Time. The travel time histogram for each approach or traffic phase represents the frequency of vehicles that completed that traffic movement journey at the intersection groping into intervals of 5 seconds within a travel time range of 0 to 1000 seconds. This is obtained from SUMO logs, by processing its trajectory data at 1 second resolution. A vehicle is said to be within the proximity of the intersection if the vehicle is on a lane that is 1-hop or 2-hop away. The travel time here tracked is the amount of time the vehicle spends in the proximity of the intersection till it exits the intersection. For each vehicle, its travel time with respect to the intersections it crosses, is extracted. These travel times are collected for each intersection and each group of lanes associated with a phase of movement and a histogram is created. The histogram varies from 0 to 1000 seconds, in buckets of 5 seconds each. Each bucket counts how many vehicles had that travel time. Eg. a count of 7 vehicles in the bucket 45-50 s along phase 2 of intersection 5, means that 7 vehicles took between 45 and 50 seconds to cross the proximity of that intersection.

V. EXPERIMENTAL RESULTS

In this section, we assess the performance of our proposed multi-tasking digital twin, referred to as MTDT. This MTDT model undergoes training on a dataset comprising 22,000 Simulation Records meticulously gathered from a diverse range of eight intersections. Additionally, we introduce two variants for comparison: MTDT-Single, trained on a dataset of 19,000 Simulation Records from a single intersection, and

MTDT-MOE, a modified version of MTDT that excludes primary modules M_{ext} and M_{inf} from the pipeline, resulting in the output of only two sets of MOEs variables, namely ql and tt , instead of the full set of variables. Lastly, we include TQAM [15] an RNN Auto-encoder as a baseline deep learning-based digital twin previously introduced in our research for the estimation of maximum queue length.

We employ widely used metrics to assess our model's performance, including Mean Absolute Error (MAE), Root Mean Square Error (RMSE), and Normalized Root Mean Squared Error (NRMSE). For travel time distribution estimation, we dissect error measures for the 60th, 75th, 85th, and 90th percentiles separately. This breakdown allows us to scrutinize the model's performance across various traffic flow dynamics within each percentile. When estimating queue length waveform time series, we opt for NRMSE over RMSE to ensure error values are relative to the scale of data. Additionally, to mitigate scale-related biases, we segment our dataset based on the magnitude of the maximum queue length logged by each *Simulation Records* and report error values for each group individually.

Table. 2 shows our proposed digital twin (MTDT) has the potential to effectively learn the joint estimation of traffic flow and MOE estimation at any intersection regardless of its lane design and configuration (topology). Although MTDT-Single is trained and evaluated at a single intersection, the error values are fairly comparable to that for MTDT except for maximum queue length estimation. This is because the formation of queues at the location of each intersection follows a more complex pattern involving several intersection-level factors. The benefit of multi-task learning can be proved by comparing the maximum queue length estimation by MTDT-MOE which is designed to estimate MOEs exclusively and MTDT-Single. Supporting the performance made for queue length by the output of primary tasks, results in better estimation results.

As shown in MTDT results, the minimal marginal increase in error values for all variables remains minimal relative to the aggregation level indicating consistent reliability and robustness in the model's performance across varying data resolutions. We also note the model exhibits enhanced performance in estimating travel time for lower quantiles of the data distribution while showing a slight improvement, particularly at the 90th quantile. This suggests that our designed digital twin is also particularly adept at capturing relatively rare or extreme patterns.

For the multifaceted and fine-grained results, our designed multi-tasking simulation stands as unique to its counterparts, thus not directly comparable to existing baselines. However, we attempt to contrast our findings with those obtained by TQAM designed to make an accurate estimation of queue length estimation in a specific approach of a specific topology of target intersection. To achieve this, we partition our data into the same queue length buckets as reported for this model and compare error values in terms of (percentage) Mean Absolute Error (MAE) in Table 3. The partitioning encompasses two groups for each of the low (L), medium

(M), and high (H) ranges of maximum queue length. These groups, ranging from L1 to H2, encompass 28%, 34%, 19%, 11%, 5%, and 3% of data samples, respectively. Our observations indicate that both MTDT and MTDT-Single exhibit comparable performance to TQAM. Specifically, MTDT outperforms TQAM in certain partitions of data where very short (0-40 meters) or long (above 200 meters) queue length tails are recorded, while MTDT-Single consistently performs equivalently or better than TQAM across nearly all partitions.

We further devise an experiment to assess the performance of our proposed digital twin under varying percentages of green time allocation to the major direction of the intersection. In this experimental setup, we focus on Phase 2/6 in the corridor-through phase, serving the *major* direction of traffic movement for all intersections. We define low, medium, and high percentages of this green time as 45-50%, 60-75%, and 75-90% of the total duration of the simulation scenario. However, the individual cycle lengths may vary due to actuated ring-and-barrier operation responding to the cycle-wise incoming traffic. After categorizing simulation records into these three groups, we evaluated the performance of MTDT and MTDT-Single across all output variables, as presented in Table 4. The findings indicate that the performance of our digital twin is fairly consistent. It excels in queue length estimation under scenarios with shorter green time allocated to the major direction, whereas travel time estimation performs better with a larger green time allocation.

VI. RELATED WORK

Existing methods of traffic flow modeling in the past literature can be categorized into linear, non-linear, machine learning, and hybrid models. With advancements in high-resolution induction loop detectors in intelligent transportation systems (ITSS), a large number of deep neural network models have been proposed for real-time and short-term traffic flow prediction raised by industries, academia, and government. In the realm of linear models, [1] proposed a localized (dynamic weight matrix) space-time autoregressive (LSTAR) model for real-time traffic prediction, [4] developed a Kalman filter (KF) for predicting real-time traffic flow of connected vehicles at urban arterials, [12] combines KF and adaptive weight allocation, and [14] formulates a consensus filter-based distributed variational Bayesian (CFBDVB) algorithm for density approximation of traffic flow and average traffic speed in a freeway.

In the realm of non-linear models, multi-kernel SVM [10] and weighted k-nearest neighbor [21] with MapReduce algorithm on Hadoop are introduced. When it comes to hybrid models, ensemble empirical mode decomposition with adaptive noise [16] and bidirectional RNN combined with road crossing vector coding [26] can be mentioned. Machine learning models in this line of research are deep learning frameworks based on the temporal convolutional network (TCN) [27], parallel computing of deep belief networks (DBNs) [25], deep characteristic learning using DBN with the multi-objective particle swarm optimization (PSO) algorithm [9]. [3] and [11] developed a deep hybrid neural

Aggregation	MTDT-Single	MTDT	MTDT-MOE
Maximum Queue Length Estimation			
	MAE RMSE	MAE RMSE	MAE RMSE
5-second buckets	4.8084 0.0885	9.6114 0.04621	9.0321 0.0297
10-second buckets	9.3787 0.08410	18.9512 0.08118	17.8554 0.0513
15-second buckets	13.8788 0.0973	27.9748 0.1012	26.4127 0.0674
20-second buckets	18.2466 0.0907	37.1869 0.1003	35.1794 0.0688
Travel Time Distribution Estimation			
	MAE RMSE 95%CI	MAE RMSE 95%CI	MAE RMSE 95%CI
60th percentile	5.50946 17.744 \pm 34.7782	5.5332 17.7440 \pm 34.7782	4.8024 15.3052 \pm 29.9981
75th percentile	5.76871 17.7987 \pm 34.8854	5.7592 18.3542 \pm 35.9742	4.8387 15.2256 \pm 29.8421
85th percentile	4.70901 13.0162 \pm 25.5117	5.7298 18.1125 \pm 35.5005	4.6844 14.8253 \pm 29.0575
90th percentile	4.1331 11.7298 \pm 22.9904	5.0685 16.3674 \pm 32.0801	3.7703 12.3752 \pm 24.2553
Exit Waveform Estimation			
	MAE RMSE 95%CI	MAE RMSE 95%CI	MAE RMSE 95%CI
5-second buckets	0.0979 0.2995 \pm 0.5870	0.1020 0.3189 \pm 0.6250	-
10-second buckets	0.1758 0.5083 \pm 0.9962	0.1844 0.5575 \pm 1.0927	-
15-second buckets	0.2477 0.6977 \pm 1.3674	0.2607 0.7761 \pm 1.5211	-
20-second buckets	0.3126 0.8683 \pm 1.7018	0.3326 0.9775 \pm 0.9775	-
Inflow Waveform Estimation			
	MAE RMSE 95%CI	MAE RMSE 95%CI	MAE RMSE 95%CI
5-second buckets	0.1145 0.3456 \pm 0.6773	0.1284 0.3785 \pm 0.7418	-
10-second buckets	0.2119 0.6005 \pm 1.1769	0.2385 0.6729 \pm 1.3188	-
15-second buckets	0.3018 0.8287 \pm 1.6242	0.3397 0.9387 \pm 1.8398	-
20-second buckets	0.3837 1.0340 \pm 2.0266	0.4367 1.1844 \pm 2.3214	-

TABLE 2: **Performance of MTDT.** The performance of our proposed digital twin is assessed across various aggregation resolutions of maximum queue length and at different quantiles of the travel time distribution. MTDT is compared to its variant (MTDT-Single and MTDT-MOE). This comparison is conducted in terms of NRMSE, RMSE, and MAE, measured in vehicle-per-bucket for Exit and Inflow waveforms, meter-per-bucket for maximum queue length, and vehicle-per-quantile for travel time distribution. Moreover, the level of confidence for estimating the relevant variable across various resolution levels is shown as 95% confidence intervals (CI).

Max. Queue Length (meter):	L1 0-40 m	L2 40-80 m	M1 80-120 m	M2 120-160 m	H1 160-200 m	H2 200+ m
MTDT	3.02 (7.5%)	6.00 (7.5%)	8.65 (7.2%)	11.34 (7.0%)	16.46 (8.2 %)	15.26 (1.5%)
MTDT-Single	2.94 (7.3 %)	5.42 (6.7 %)	7.27 (6.0 %)	9.16 (5.7 %)	11.05 (5.5 %)	9.80 (0.9 %)
TQAM	2.90 (7.3%)	5.50 (6.9%)	7.00 (5.8%)	9.00 (5.6%)	11.60 (5.8%)	18.10 (1.8%)

TABLE 3: **Evaluation at various maximum queue length ranges** A comparative analysis is conducted between MTDT, MTDT-Single, and TQAM for queue length waveform time series estimation across different queue length buckets. The assessment is based on MAE and the percentage of MAE relative to the upper range within each bucket, measured in meters per 5-second time resolution.

Task	Green Time (percentage):	Error Measure		
		Low 45-60 %	Medium 60-75 %	High 75-90 %
MTDT-Single				
Exit Waveform	MAE	0.0106	0.0963	0.0936
	RMSE	0.3556	0.3121	0.3439
Inflow Waveform	MAE	0.1518	0.3632	0.4113
	RMSE	0.1199	0.320	0.3430
Maximum Queue Length	MAE	6.0780	5.9700	4.5635
	NRMSE	0.2071	0.1392	0.0778
Travel Time Distribution	MAE	1.4173	2.8246	3.1870
	RMSE	4.9942	9.7389	10.827
MTDT				
Exit Waveform	MAE	0.0905	0.09108	0.0926
	RMSE	0.3288	0.0800	0.3052
Inflow Waveform	MAE	0.1204	0.1151	0.1101
	RMSE	0.4052	0.3811	0.3438
Maximum Queue Length	MAE	12.105	11.946	8.6872
	NRMSE	0.4243	0.2780	0.1557
Travel Time Distribution	MAE	0.0915	2.3671	3.0768
	RMSE	8.4421	9.0937	10.735

TABLE 4: **Evaluation at various green time allocations.** The performance of the model is evaluated at different plit of data based on corridor-through green time percentage buckets.

network combined with CNN and LSTM using trajectory data for better accuracy and robustness of forecasting performance, while [23] combined GCN and attention mechanism for lane-wise and topology invariant traffic flow estimation.

Some literature integrates operation performance forecasting in traffic signal control of intersections and networks. For example, [13] makes use of graph mining and trajectory data mining methods to provide interactive evaluation and exploration of the various MOEs, while [2] proposed a safety-enhanced residual reinforcement learning method (SafeLight) to integrate safety conditions in traffic signal control by integrating knowledge using multi-objective loss function and reward shaping, and [6] proposed a metaheuristic-based method for intelligent traffic control using Genetic Algorithm (GA) and differential evolution (DE) to improve the level of service (LOS) i.e. delay optimization of intersection through optimizing the signal timing plan.

VII. CONCLUSIONS AND FUTURE WORK

In this paper, we demonstrate the effectiveness of multi-tasking as a learning paradigm for deep learning-based digital twins. We introduce a Multi-Task Deep Learning Digital Twin that utilizes multiple convolutions over graphs and time series. This approach can successfully perform a variety of related traffic simulation tasks for urban intersections with arbitrary topologies and characteristics. Our findings highlight the benefits of the multi-task learning approach in the design of our digital twin, not only for secondary tasks whose inputs rely on the output of primary tasks but also for primary tasks to generalize and enhance their performance through shared learned representations and joint optimization. Furthermore, we design two experiments to specifically illustrate how the model's performance varies across different partitions of data when simulation scenarios are segmented based on signal timing plans or maximum recorded queue length. The results underscore the consistency and robustness of our approach across different experiments. Moreover, we discuss the lack of a baseline due to the uniqueness and comprehensiveness of our approach. However, we show it still outperforms in individual tasks compared to some previously introduced digital twins specialized for specific tasks.

Looking ahead, there are several aspects of future work in this research that we briefly discuss in the following.

MTDT can serve as a valuable tool to assist traffic decision-makers in comprehending the potential impact of alterations to signal timing plans and proposed changes to road geometry. Additionally, it can be seamlessly integrated into signal timing optimization frameworks or expanded from isolated intersections to corridors and networks which will be a focal point of our future endeavors.

VIII. ACKNOWLEDGMENTS

The work was supported in part by NSF CNS 1922782. The opinions, findings, and conclusions expressed in this publication are those of the authors and not necessarily those of NSF. The authors also acknowledge the University of Florida Research Computing for providing computational resources and support that have contributed to the research results reported in this publication.

REFERENCES

- [1] J. Chen, D. Li, G. Zhang, and X. Zhang. Localized space-time autoregressive parameters estimation for traffic flow prediction in urban road networks. *Applied Sciences*, 8(2):277, 2018.
- [2] W. Du, J. Ye, J. Gu, J. Li, H. Wei, and G. Wang. Safelight: A reinforcement learning method toward collision-free traffic signal control. In *Proceedings of the AAAI Conference on Artificial Intelligence*, volume 37, pages 14801–14810, 2023.
- [3] Z. Duan, Y. Yang, K. Zhang, Y. Ni, and S. Bajgain. Improved deep hybrid networks for urban traffic flow prediction using trajectory data. *Ieee Access*, 6:31820–31827, 2018.
- [4] A. Emami, M. Sarvi, and S. Asadi Bagloee. Using kalman filter algorithm for short-term traffic flow prediction in a connected vehicle environment. *Journal of Modern Transportation*, 27:222–232, 2019.
- [5] M. Fang, L. Tang, X. Yang, Y. Chen, C. Li, and Q. Li. Ftpg: A fine-grained traffic prediction method with graph attention network using big trace data. *IEEE Transactions on Intelligent Transportation Systems*, 23(6):5163–5175, 2021.
- [6] A. Jamal, M. Tauhidur Rahman, H. M. Al-Ahmadi, I. Ullah, and M. Zahid. Intelligent intersection control for delay optimization: Using meta-heuristic search algorithms. *Sustainability*, 12(5):1896, 2020.
- [7] Y. Karnati, R. Sengupta, and S. Ranka. Intertwin: Deep learning approaches for computing measures of effectiveness for traffic intersections. *Applied Sciences*, 11(24):11637, 2021.
- [8] Y. LeCun, L. Bottou, Y. Bengio, and P. Haffner. Gradient-based learning applied to document recognition. *Proceedings of the IEEE*, 86(11):2278–2324, 1998.
- [9] L. Li, L. Qin, X. Qu, J. Zhang, Y. Wang, and B. Ran. Day-ahead traffic flow forecasting based on a deep belief network optimized by the multi-objective particle swarm algorithm. *Knowledge-Based Systems*, 172:1–14, 2019.
- [10] X. Ling, X. Feng, Z. Chen, Y. Xu, and H. Zheng. Short-term traffic flow prediction with optimized multi-kernel support vector machine. In *2017 IEEE Congress on Evolutionary Computation (CEC)*, pages 294–300. IEEE, 2017.
- [11] D. Ma, B. Sheng, S. Jin, X. Ma, and P. Gao. Short-term traffic flow forecasting by selecting appropriate predictions based on pattern matching. *IEEE Access*, 6:75629–75638, 2018.
- [12] M. Ma, S. Liang, H. Guo, and J. Yang. Short-term traffic flow prediction using a self-adaptive two-dimensional forecasting method. *Advances in Mechanical Engineering*, 9(8):1687814017719002, 2017.
- [13] A. Nematicchari, T. Pechlivanoglou, and M. Papagelis. Evaluating and forecasting the operational performance of road intersections. In *Proceedings of the 30th International Conference on Advances in Geographic Information Systems*, pages 1–12, 2022.
- [14] B. Safarinejad and M. E. Estahbanati. Consensus filter-based distributed variational bayesian algorithm for flow and speed density prediction with distributed traffic sensors. *IEEE Systems Journal*, 11(4):2939–2948, 2015.
- [15] R. Sengupta, Y. Karnati, A. Rangarajan, and S. Ranka. Tqam: Temporal attention for cycle-wise queue length estimation using high-resolution loop detector data. In *2021 IEEE International Intelligent Transportation Systems Conference (ITSC)*, pages 3313–3320. IEEE, 2021.
- [16] X. Tian, D. Yu, X. Xing, S. Wang, and Z. Wang. Hybrid short-term traffic flow prediction model of intersections based on improved complete ensemble empirical mode decomposition with adaptive noise. *Advances in Mechanical Engineering*, 11(4):1687814019841819, 2019.
- [17] P. Veličković, G. Cucurull, A. Casanova, A. Romero, P. Lio, and Y. Bengio. Graph attention networks. *arXiv preprint arXiv:1710.10903*, 2017.
- [18] G. Vigos, M. Papageorgiou, and Y. Wang. Real-time estimation of vehicle-count within signalized links. *Transportation Research Part C: Emerging Technologies*, 16(1):18–35, 2008.
- [19] J. L. Wolf, W. H. Bachman, M. S. Oliveira, J. A. Auld, A. Mohammadian, P. S. Vovsha, and J. Zmud. *Applying GPS data to understand travel behavior*, volume 1. Transportation Research Board, 2014.
- [20] M. A. Wright, S. F. Ehlers, and R. Horowitz. Neural-attention-based deep learning architectures for modeling traffic dynamics on lane graphs. In *2019 IEEE Intelligent Transportation Systems Conference (ITSC)*, pages 3898–3905. IEEE, 2019.
- [21] D. Xia, B. Wang, H. Li, Y. Li, and Z. Zhang. A distributed spatial-temporal weighted model on mapreduce for short-term traffic flow forecasting. *Neurocomputing*, 179:246–263, 2016.
- [22] J. Yao and K. Tang. Cycle-based queue length estimation considering spillover conditions based on low-resolution point detector data. *Transportation research part C: emerging technologies*, 109:1–18, 2019.
- [23] N. Yousefzadeh, R. Sengupta, Y. Karnati, A. Rangarajan, and S. Ranka. Graph attention network for lane-wise and topology-invariant intersection traffic simulation. *arXiv preprint arXiv:2404.07446*, 2024.
- [24] N. Yousefzadeh, M. T Thai, and S. Ranka. A comprehensive survey on multilayered graph embedding. 2023.
- [25] L. Zhao, Y. Zhou, H. Lu, and H. Fujita. Parallel computing method of deep belief networks and its application to traffic flow prediction. *Knowledge-Based Systems*, 163:972–987, 2019.
- [26] S. Zhao, Q. Zhao, Y. Bai, and S. Li. A traffic flow prediction method based on road crossing vector coding and a bidirectional recursive neural network. *Electronics*, 8(9):1006, 2019.
- [27] W. Zhao, Y. Gao, T. Ji, X. Wan, F. Ye, and G. Bai. Deep temporal convolutional networks for short-term traffic flow forecasting. *Ieee Access*, 7:114496–114507, 2019.